Hole and electron contributions to the transport properties of $Ba(Fe_{1-x}Ru_x)_2As_2$ single crystals

F. Rullier-Albenque,[1,*] D. Colson,[1] A. Forget,[1] P. Thuéry,[2] and S. Poissonnet[3]
[1]*Service de Physique de l'Etat Condensé, Orme des Merisiers, IRAMIS, CEA-Saclay (CNRS URA 2464), 91191 Gif sur Yvette Cedex, France*
[2]*SIS2M, LCCEf, IRAMIS, CEA, CNRS UMR 3299, 91191 Gif-sur-Yvette Cedex, France*
[3]*Service de Recherches de Métallurgie Physique, CEA-Saclay, 91191 Gif sur Yvette Cedex, France*
(Received 28 March 2010; revised manuscript received 7 May 2010; published 2 June 2010)

We report a systematic study of structural and transport properties in single crystals of $Ba(Fe_{1-x}Ru_x)_2As_2$ for x ranging from 0 to 0.5. The isovalent substitution of Fe by Ru leads to an increase in the a parameter and a decrease in the c parameter, resulting in a strong increase in the As-Fe-As angle and a decrease in the As height above the Fe planes. On Ru substitution, the magnetic order is progressively suppressed and superconductivity emerges for $x \geq 0.15$ with an optimal $T_c \simeq 20$ K at $x=0.35$ and coexistence of magnetism and superconductivity between these two Ru contents. Moreover, the Hall coefficient R_H, which is always negative and decreases with temperature in $BaFe_2As_2$, is found to increase here with decreasing T and even changes sign for $x \geq 0.20$. For $x_{Ru}=0.35$, photoemission studies have shown that the number of holes and electrons are similar with $n_e=n_h \simeq 0.11$ carriers/Fe, that is twice larger than found in $BaFe_2As_2$ [V. Brouet, F. Rullier-Albenque, M. Marsi, B. Mansart, J. Faure, L. Perfetti, A. Taleb-Ibrahimi, P. Le Fèvre, F. Bertran, A. Forget, and D. Colson, arXiv:1002.4952 (unpublished)]. Using this estimate, we find that the transport properties of $Ba(Fe_{0.65}Ru_{0.35})_2As_2$ can be accounted for by the conventional multiband description for a compensated semimetal. In particular, our results show that the mobility of holes is strongly enhanced on Ru addition and overcomes that of electrons at low temperature when $x_{Ru} \geq 0.15$.

DOI: 10.1103/PhysRevB.81.224503 PACS number(s): 74.70.Xa, 74.62.Bf, 74.25.Dw, 74.25.fc

I. INTRODUCTION

In iron pnictides the appearance of high-T_c superconductivity induced by carrier doping or pressure in close proximity to the antiferromagnetic phase appears very similar to the behavior of cuprates and heavy-fermion superconductors and has been taken as the signature of unconventional superconductivity in these compounds. It seems now well established that magnetism and superconductivity (SC) are intimately correlated and directly connected to the peculiar features of the electronic structures of these compounds. More precisely the changes in the Fermi surface and the modifications of the nesting conditions between hole and electron pockets have been proposed to be the driving force for the suppression of antiferromagnetism and the emergence of superconductivity with a sign reversing $s_\pm$ symmetry.[1]

So far a lot of studies have been devoted to the 122 family as superconductivity can be induced not only by doping with holes[2] or electrons[3,4] but also through chemical or physical pressure.[5,6] Several investigations have been done in order to find out a relevant parameter allowing to explain the modifications of the electronic structure and the emergence of superconductivity in these different systems. On one hand, it has been argued that structural modifications could be more important than doping in achieving superconductivity, either through the height of As with respect to Fe planes[7] or the value of the As-Fe-As bonding tetrahedral angle.[8] On the other hand, in the case of electron-doped compounds, the steric effect due to different atomic substitutions in the Fe planes has been shown to be of minor importance compared to the effect of doping.[9] Let us note that the very low level of substitution sufficient to induce SC in this latter case is compatible with weak structural distortion effects. However, in the case of hole doping for which large substitution level (around 35%) is necessary to get the optimal T_c, it seems more difficult to distinguish between doping and structural modifications.

Studies of transport properties are *a priori* one of the simplest way to investigate the modifications of the electronic structure. However the situation in the 122 family is far from being clear. In the undoped $BaFe_2As_2$ parent, for which electron and hole contents are identical ($n=n_e=n_h$), it is found quite surprisingly that the Hall coefficient R_H is always negative, indicating that electrons dominate the transport properties both above and below the structural/magnetic transition at $T \simeq 140$ K. The same observation has been found for Co-doped samples all over the phase diagram.[10,11] For all these compounds, it seems that the holes are highly scattered and thus not directly visible in the transport properties.[12] The case of isovalent substitution of As by P is even more intriguing as a negative Hall coefficient is also found for all P contents.[13] In fact, positive R_H have been only reported for K- and Cr-doped $BaFe_2As_2$, as naturally expected for hole-doped compounds.[14,15]

The isovalent substitution of Fe by Ru provides another alternative to study the modifications of the transport properties in the 122 family. It has been shown recently on polycrystalline samples[16,17] that the introduction of Ru suppresses the spin-density wave (SDW) magnetic order and induces SC. Density-functional calculations show that Ru substitution does not induce any charge imbalance between the bands and no additional bands related to Ru appear at the Fermi level.[18] However a negative Hall coefficient with a weak T dependence has also been reported for polycrystalline $BaFe_{1.25}Ru_{0.75}As_2$.[16]

Here we report on structural, resistivity and Hall effect data obtained on single crystals of $Ba(Fe_{1-x}Ru_x)_2As_2$ for x

ranging from 0 to 0.5. As reported previously, we confirm the suppression of the magnetostructural transition and the emergence of SC for $x \gtrsim 0.15$ with an optimal $T_c \sim 20$ K at $x \simeq 0.35$. We find that the lattice parameter a (c), respectively, increases (decreases) on Ru addition, so that a/c increases markedly. As for the transport properties, our Hall effect measurements evidence the contribution of both holes and electrons in the transport properties, as the Hall coefficient changes sign from negative to positive with decreasing temperature. On the other hand, angle-resolved photoemission spectroscopy (ARPES) measurements performed on similar single crystals with $x=0.35$ (Ref. 19) confirm that Ru-substituted $BaFe_2As_2$ behave as a compensated metal with essentially the same number of holes and electrons, i.e., $n=n_e=n_h \simeq 0.11$ carriers/Fe. Assuming a two-band model to describe the transport properties, we show that it is possible here to disentangle the respective contributions of electrons and holes. Quite surprisingly the deduced electron and hole resistivity curves display similar T dependences as those found, respectively, for Co-doped and K-doped $BaFe_2As_2$ at optimal doping. Their evolutions with Ru content show that the mobility of holes is more affected than that of electrons. The strong modification of the electronic structure of $BaFe_2As_2$ with Ru substitution revealed by ARPES (Ref. 19) might be the key factor for governing these properties.

II. SAMPLES AND STRUCTURAL MEASUREMENTS

Single crystals of $Ba(Fe_{1-x}Ru_x)_2As_2$ with Ru contents x ranging from 0 to 0.50 were grown using a FeAs/Ru+As self-flux method. Small Ba chunks, FeAs powder, and RuAs (or Ru+As) powders were mixed in the ratio Ba:(FeAs+RuAs)=1:4. Starting products were put in an alumina crucible and sealed in an evacuated quartz tube which was put into a tubular furnace. The samples were heated to 1180 °C, held at this temperature for 4 h, cooled slowly first to 1000 °C (3–6 °C/h) and then more rapidly to room temperature. Clean crystals of typical dimensions $0.5 \times 0.5 \times 0.05$ mm^3 were mechanically extracted from the flux. It is worth pointing out here that it is very difficult to get homogeneous single crystals for $x_{Ru} \geq 0.2$, probably due to the very high melting temperatures of Ru and RuAs with respect to that of FeAs. Consequently, the Ru composition of each studied crystal has been determined with a Camebax SX50 electron microprobe in several spots of the surfaces. The structural properties were characterized by single crystal x-ray diffraction on very thin platelets ($\sim 0.10 \times 0.05 \times 0.01$ mm^3). The data were collected at room temperature on a Nonius Kappa-CCD area detector diffractometer[20] using graphite-monochromated Mo $K\alpha$ radiation ($\lambda=0.71073$ Å). The data (combinations of φ and ω scans giving complete data sets up to $\theta=27.4°$ at least and a minimum redundancy of 4 for 90% of the reflections) were processed with HKL2000.[21] Absorption effects were corrected empirically with the program SCALEPACK.[21] The structures were refined in the tetragonal space group $I4/mmm$ by full-matrix least squares on F2 with SHELXL-97.[22] All the atoms were refined with anisotropic displacement parameters, so that ten parameters were refined on ~100 independent reflections. Fe and Ru were constrained to retain the same displacement parameters, which enabled to refine the Ru content x. The final R_1 indices are in the range 0.020–0.042 and the wR_2 values in the range 0.043–0.113.[23]

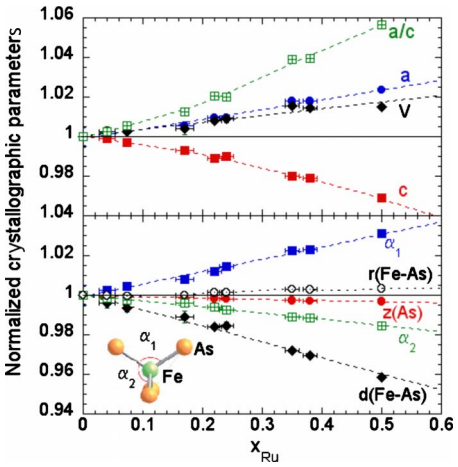

FIG. 1. (Color online) (a) Variation in the lattice parameters a and c, their ratio a/c and the unit-cell volume V, normalized to their values for the undoped compound, as a function of the Ru content x (determined by x-ray diffraction). (b) The same for different crystallographic parameters: the two As-Fe-As tetrahedral angles, α_1 and α_2, the c-axis coordinate of As, z_{As}, the Fe-As interatomic distance r(Fe-As) and the height of As above Fe layers, $d_{Fe\text{-}As}$.

The relative lattice parameters are plotted in Fig. 1 versus the refined value of x_{Ru} while numerical data are reported in Table I for $x=0$ (undoped $BaFe_2As_2$) and $x=0.38$ (optimal doping). On substitution, the a parameter and the cell volume increase while the c parameter decreases in about the same proportion (by 2–3 % for $x=0.5$) in agreement with data on polycrystalline samples.[16] The main effect of Ru substitution is thus to strongly increase the ratio (a/c). This results in a strong increase in the As-Fe-As tetrahedral bonding angle α_1 displayed in Fig. 1(b) which varies by 4% for $x=0.5$. Moreover, while the z parameter of As and the Fe-As interatomic distance are nearly unaffected by Ru substitution, the vertical

TABLE I. Crystallographic data taken at room temperature for the parent and Ru-substituted ($x=0.38$) $Ba(Fe_{1-x}Ru_x)_2As_2$. The space group of both compounds is $I4/mmm$ and the atomic coordinates are: Ba(0,0,0), Fe/Ru(0.5,0,0.25), and As (0,0,z). α_1 and α_2 are the bonding tetrahedral angles as sketched in Fig. 1.

	$x=0$	$x=0.38$
a (Å)	3.9633(4)	4.0342(5)
c (Å)	13.022(2)	12.749(2)
V (Å^3)	204.55(4)	207.49(5)
z_{As}	0.35424(6)	0.35328(8)
$\alpha_1 \times 2$ (deg)	111.18(3)	113.73(4)
$\alpha_2 \times 4$ (deg)	108.624(15)	107.39(2)
As height (Å)	1.3575	1.3165
Fe-As interatomic distance (Å)	2.402(2)	2.409(2)
FeAs layer spacing (Å)	3.796	3.741

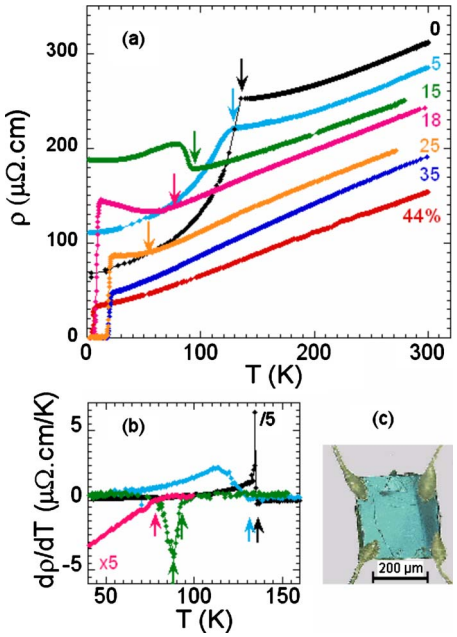

FIG. 2. (Color online) (a) Temperature dependence of the in-plane resistivity $\rho(T)$ of $Ba(Fe_{1-x}Ru_x)_2As_2$ single crystals. The arrows point the strong anomalies in the $\rho(T)$ curves that signal the occurrence of the magnetostructural transition. They are determined more precisely in (b) which shows $d\rho/dT$ versus T. For the $x=0.26$ sample, the arrow corresponds to the maximum of the Hall coefficient as explained in the text. (c) Picture of a typical sample mounted in the van der Pauw configuration.

distance of As from the Fe layers decreases due to the strong c decrease. These tendencies can be explained quite naturally by the larger size of Ru^{2+} compared to Fe^{2+} which expands the distances within Fe-Ru planes. Also the larger delocalization of the Ru $4d$ orbitals with respect to Fe $3d$ reinforces the hybridization with As and then reduces the c-axis parameter.[18] Let us note that the variation in the lattice parameters on Ru substitution displays the same trend as that observed in electron-doped $BaFe_2As_2$ compounds, although the incidence on the structure appears much weaker in this latter case.[9] However it is at odds to the tendency found for hole doping or pressure[8,24] for which both a and the As-Fe-As α_1 angle are found to decrease.

III. RESISTIVITY MEASUREMENTS AND PHASE DIAGRAM

Transport measurements were performed on crystals cleaved to thicknesses lower than 20 μm and cut to get square samples with $\sim 0.2-0.3$ mm width [see Fig. 2(c)]. Contacts were done with silver epoxy in the van der Pauw configuration.[25]

Figure 2(a) shows the $\rho(T)$ curves as a function of Ru content. In $BaFe_2As_2$, the combined structural and magnetic (S-M) transition at $T_0=137$ K is signalled by a decrease in the resistivity.[26] For the lowest Ru content $x=0.05$ studied here, we still observe a resistivity decrease at the S-M transition but with a much wider transition as seen in Fig. 2(b), which shows the resistivity derivative $d\rho/dT$. Then for larger

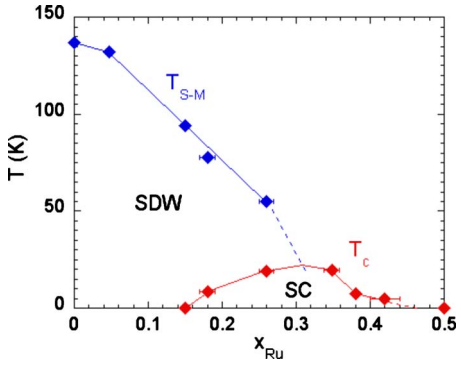

FIG. 3. (Color online) Phase diagram of the $Ba(Fe_{1-x}Ru_x)_2As_2$ system showing the evolution of the structural-magnetic transition $T_{S\text{-}M}$ and critical temperatures T_c versus Ru content x_{Ru}. Values of T_c are taken at the midpoint of superconducting transitions. The sample with $x=0.5$ is no longer superconducting as shown by superconducting quantum interference device magnetometer measurements.

Ru contents, the resistive signature of the S-M transition, determined by the deviations in $d\rho/dT$, changes shape towards a steplike increase in the resistivity as observed in electron-doped compounds. In contrast, let us point out that the S-M transition is always signaled by a decrease in the resistivity in polycrystalline samples,[16,17] which might be related to inhomogeneities in the samples or directional averaging due to different in-plane and out-of-plane resistivity variations at the S-M transition. For $x=0.15$, it is possible to distinguish between structural and magnetic transitions, using the same criteria based on the variation in $d\rho/dT$ as proposed for Co-doped samples [arrows in Fig. 2(b)].[4,27] This would give 95 K and 88 K, respectively, for T_S and T_{SDW}. For the other samples, this distinction is not possible and microscopic investigations are needed to determine the respective values of T_S and T_{SDW}.

Superconductivity appears for $x \geq 0.15$ and a maximum T_c of 19.5 ± 0.5 K is found for $x=0.35$, in excellent agreement with the value found for polycrystalline samples of Ru-substituted $Ba(Sr)Fe_2As_2$.[16,17] The T-x phase diagram obtained for $Ba(Fe_{1-x}Ru_x)_2As_2$ is displayed in Fig. 3. One can notice that the superconducting region is rather small, particularly in the "overdoped" region where T_c is found to drop rapidly beyond $x=0.35$. As in the doped compounds, coexistence between magnetism and superconductivity is clearly evidenced with the optimal T_c occurring when long-range magnetic order is fully suppressed. This points here again to the importance of spin fluctuations for superconductivity in these systems. From these resistivity data, it is not possible to know whether the coexistence between magnetism and superconductivity occurs at the atomic scale like in Co-doped samples[28] or comes from phase segregation as observed in K-doped samples[29,30] and further studies at the miscoscopic level are needed to assess this point.

We find here that superconductivity is induced on Ru addition while the $FeAs_4$ tetrahedra become strongly distorted as both α_1 and α_2 angles deviate from 109.5°, the ideal tetrahedral value. This observation conflicts with the claim that the regularization of tetrahedra is the optimal condition for

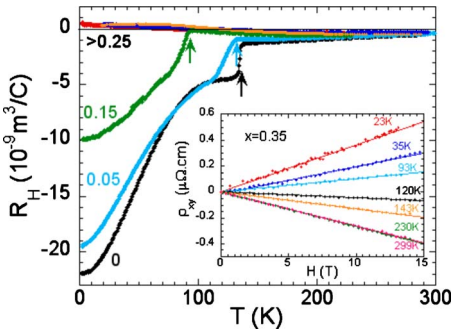

FIG. 4. (Color online) T dependence of the Hall coefficient $R_H(T)$ for various compositions. The temperatures at which R_H starts decreasing due to the apparition of the M-S transition correspond exactly to those where anomalies are seen in the resistivity curves (arrows). The inset shows that the Hall resistivity ρ_{xy} of the $x=0.35$ sample is linear in magnetic field up to 14 T whatever T. A sign change in the slope occurs between 93 and 120 K.

achieving superconductivity in pnictides.[8,31,32] Let us also note that Ru substitution in the 1111 PrFeAsO compound induces similar crystallographic modifications as those observed here in $BaFe_2As_2$ (Ref. 33) with suppression of the magnetic order but no apparition of superconductivity.

On another hand, band-structure calculations have pointed out the important impact of the vertical distance $d_{\text{Fe-As}}$ on the Fermi-surface topology of iron pnictices.[34] Mizugushi *et al.*[7] have recently shown that a striking correlation between T_c and the Fe-As distance is followed by a lot of different FeAs superconductors. This plot is symmetric with a peak around $d_{\text{Fe-As}}=1.38$ Å. We find that the point corresponding to $Ba(Fe_{1.62}Ru_{0.35})_2As_2$ ($d_{\text{Fe-As}}=1.3165$ Å) and $T_c \simeq 20$ K is on the left branch while the one for pressure or hole doping is located on the right one. Even though other factors are clearly at play for governing the apparition of superconductivity in the 122 family, the relationship between the values of T_c and $d_{\text{Fe-As}}$ may provide a helpful hint to understand the modifications of the electronic properties.

IV. HALL EFFECT AND ANALYSIS OF TRANSPORT PROPERTIES

The temperature dependences of the Hall coefficient R_H are displayed in Fig. 4 for different Ru concentrations. In the paramagnetic state of the samples, we have checked that the Hall resistivity is always linear in field up to 14 T, which allows to define R_H unambiguously.[35] This linearity is illustrated in the inset of Fig. 4 for the $x=0.35$ sample. The strong reduction in the Hall coefficient at the S-M transition is well correlated to the anomalies seen in $d\rho/dT$ and represented by arrows in the figure. It can be associated, as in the undoped parent, to the reduction in carrier density due to the reconstruction and/or partial gaping of the Fermi surfaces. The fact that R_H remains negative indicates that electrons still dominate the transport properties in the magnetic phase of Ru-substituted samples.

Figure 5(a) shows an enlarged view of the evolution of the Hall coefficient in the paramagnetic phase. For comparison, we have also plotted in Fig. 5(b) similar data obtained

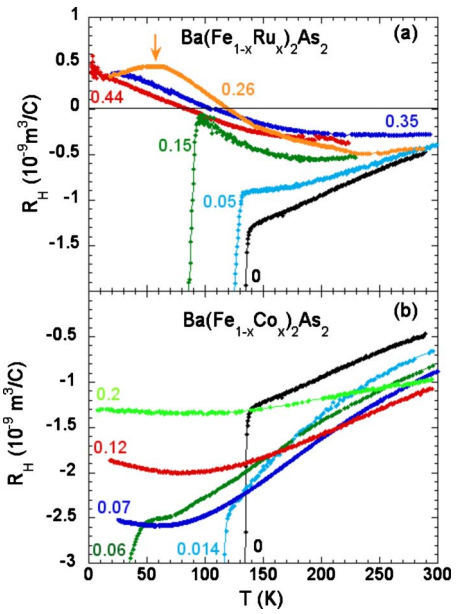

FIG. 5. (Color online) T dependence of the Hall coefficient $R_H(T)$ in the vicinity of $R_H=0$ for (a) $Ba(Fe_{1-x}Ru_x)_2As_2$ and (b) $Ba(Fe_{1-x}Co_x)_2As_2$, from Ref. 10.

for $Ba(Fe_{1-x}Co_x)_2As_2$ at various dopings.[10] In this latter case, R_H is always found negative, indicating that the contribution of electrons dominates the transport properties. However an opposite trend appears as soon as Ru is added to $BaFe_2As_2$. For $x=0.15$, R_H nearly reaches zero before dropping at the S-M transition and for higher Ru contents, a change in sign of R_H occurs at low temperature. In particular for the $x \sim 0.25$ sample, we observe that R_H increases and becomes positive on cooling and then appears to slightly decrease again for $T \leq 50$ K. This can be related to the flattening of the $\rho(T)$ curves observed in the same temperature range and this is for us the sign that the S-M transition takes place at $T \simeq 50$ K in this sample.

In multiband systems, it is well known that a temperature variation in the Hall coefficient can be assigned to different variations in hole and electron mobilities with temperature. The observation of a sign change in R_H in $Ba(Fe_{1-x}Ru_x)_2As_2$ indicates that holes and electrons contribute similarly to the transport in a large temperature range. More precisely ARPES data on crystals with 35% Ru (Ref. 19) have shown that the number of holes and electrons are similar, i.e., $n=n_e=n_h \simeq 0.11$ carriers/Fe. It is worth pointing out that this value is significantly larger than that determined by ARPES in the paramagnetic phase of $BaFe_2As_2$: $n=0.06(2)$ carriers/Fe,[36] which indicates that even though Ru is isovalent of Fe, it induces important modifications of the electronic structure. This equality of n_e and n_h is consistent with the observation that the Hall resistivity ρ_{xy} is always linear with magnetic field. Indeed in a two-band model, the Hall resistivity ρ_{xy} can be written out as

$$\rho_{xy} = \frac{1}{e}\frac{n_h\mu_h^2 - n_e\mu_e^2 + (\mu_h\mu_e)^2(n_h - n_e)H^2}{(n_h\mu_h + n_e\mu_e)^2 + (\mu_h\mu_e)^2(n_h - n_e)^2H^2}H, \qquad (1)$$

where $\mu_h=|e|\tau_h/m_h$ ($\mu_e=|e|\tau_e/m_e$) are the mobilities of holes (electrons) and τ_h (τ_e) and m_h (m_e) their relaxation rates and

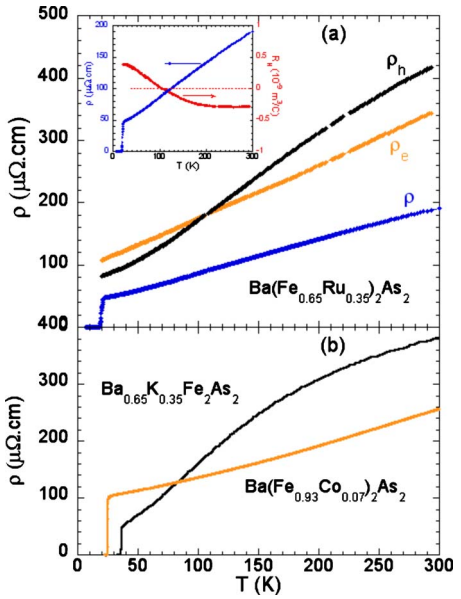

FIG. 6. (Color online) (a) Respective resistivities of electrons and holes for $Ba(Fe_{0.65}Ru_{0.35})_2As_2$ obtained from the data of resistivity and Hall coefficient using Eqs. (2) and (3) with $n_e=n_h=0.11$, as given by ARPES measurements on similar samples (Ref. 19). The raw data for resistivity and Hall coefficient are recalled in the inset. (b) The resistivity curves for $Ba(Fe_{0.93}Co_{0.07})_2As_2$ (Ref. 10) and $Ba_{0.65}K_{0.35}Fe_2As_2$ (Ref. 14) are given for comparison.

effective masses. For $n_e=n_h=n$, the H^2 term in the numerator and denominator of Eq. (1) vanishes resulting in linear variation in ρ_{xy} with H, whatever H and T.

Knowing n, it is then straightforward to deduce the respective contributions of electrons and of holes to the transport for the $x=0.35$ sample from the resistivity and Hall coefficient data, using

$$1/\rho = \sigma = \sigma_e + \sigma_h \tag{2}$$

and

$$R_H = \frac{1}{ne}\frac{\mu_e - \mu_h}{\mu_e + \mu_h} = \frac{1}{ne}\frac{\sigma_e - \sigma_h}{\sigma_e + \sigma_h}. \tag{3}$$

The resulting resistivity curves obtained for electrons and holes are displayed in Fig. 6(a). It is striking to see that the shapes of the curves resemble those obtained, respectively, for electron- and hole-doped $BaFe_2As_2$ at optimal doping. These similarities give strong support to the validity of the decomposition using the two-band model. One can also notice that $\rho_h(T)$ displays a nearly T^2 dependence as in $Ba_{0.65}K_{0.35}Fe_2As_2$ (Ref. 14) while $\rho_e(T)$ exhibits a nearly linear T dependence up to 150 K as in $Ba(Fe_{0.93}Co_{0.07})_2As_2$.[10] These temperature variations appear then tightly connected to the type of carriers—hole or electrons—and indicate an intrinsic disparity between their respective properties.

It has been suggested that the linear T dependence of resistivity found in $Ba(Fe_{1-x}Co_x)_2As_2$ or $BaFe_2As_{1-x}P_x$ near optimal doping might be a general property of unconventional superconductors near a SDW instability[37] or a signature of non-Fermi-liquid behavior.[13] The observation of a linear behavior for the electrons and *not for the holes* in the same sample clearly addresses the question of the real physical origin of this linearity. In $Ba(Fe_{1-x}Co_x)_2As_2$, the analysis of combined data of resistivity and Hall effect for $n_e>n_h$ led us to suggest that this linearity comes from an artifact due to a small variation in n_e with temperature and that the scattering rates obey the T^2 behavior expected for Fermi liquids.[10]

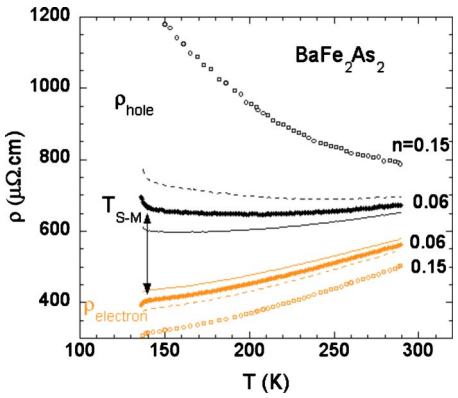

FIG. 7. (Color online) Respective resistivities of electrons and holes for $BaFe_2As_2$ in the paramagnetic phase ($T>T_{S\text{-}M}$) obtained from resistivity and Hall coefficient data using Eqs. (2) and (3) using different estimates for the carrier number. The full symbols are for $n=n_e=n_h=0.06$ carriers/Fe as determined by ARPES measurements (Ref. 36) while the full and dotted lines correspond to the extremal values of n due to the ± 0.02 error bar. The empty symbols are for the LDA estimate $n=n_e=n_h=0.15$ carriers/Fe.

V. CONTRIBUTION OF ELECTRONS AND HOLES TO THE ELECTRONIC TRANSPORT

The most striking result of this study is that electrons and holes contribute similarly to the transport in $Ba(Fe_{1-x}Ru_x)_2As_2$. This is in contrast to the observations of negative Hall coefficient in the undoped parent[10,11] or on isovalent exchange of As by P.[13] An important question is thus to understand why the holes are more scattered than the electrons in these latter cases.

In $BaFe_2As_2$, ARPES data have shown that the number of carriers is $n_e=n_h=0.06(2)$ carriers/Fe, about twice smaller than the estimate given by LDA calculations.[36,38] We have then performed the same decomposition for $BaFe_2As_2$ in the paramagnetic phase, i.e., for $T>140$ K, as done above, using either $n=0.06(2)$ carriers/Fe or $n=0.15$ carriers/Fe (Fig. 7). It is clear that the results are much more sensitive to the actual value of n for the holes than for the electrons: the electron resistivity always displays a metallic behavior with similar values while the hole one tends toward a semiconducting behavior when approaching the magnetostructural transition. The disparity between the two types of carriers appears more or less pronounced depending on the value taken for the carrier number.

It has been suggested that spin fluctuations due to interband electron-hole scattering might play a crucial role to explain the asymmetric behaviors of holes and electrons in undoped and electron-doped $BaFe_2As_2$.[11] On the contrary, our Hall coefficient data displayed in Fig. 5(a) for different

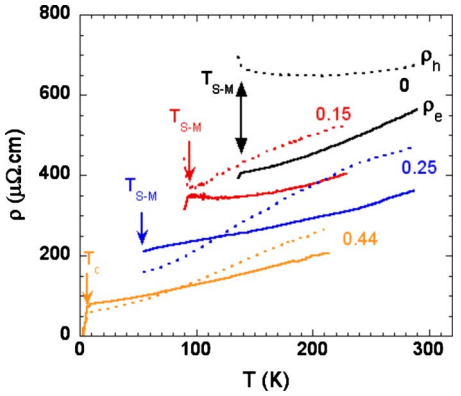

FIG. 8. (Color online) Same decompositions as that performed in Fig. 6(a) for different Ru contents, assuming a linear variation in the number of carriers with x: $n=0.06+0.14x$ carriers/Fe. Full and dotted lines are for ρ_e and ρ_h, respectively. For the sake of clarity, the data corresponding to $x=0.35$ [Fig. 6(a)] are not reported in this plot.

Ru contents seem to indicate that the proximity of magnetism does not play here an important role on the respective mobilities of the carriers. This is more visible in Fig. 8 where the decompositions in ρ_e and ρ_h are reported for different Ru contents, assuming a linear variation in n with x_{Ru}.

Even though this analysis is tentative, it gives some trends on the evolution of the transport properties of $BaFe_2As_2$ on Ru addition. In particular, one can notice that the decrease in hole and electron resistivities cannot be entirely explained by the increase in n. This therefore points to a concomitant increase in their respective mobilities. As shown by ARPES measurements on the $x=0.35$ sample, Ru substitution strongly modifies the electronic structure with respect to that of undoped $BaFe_2As_2$: not only the number of carriers has doubled but also the Fermi velocities have increased by a factor 2 or 3.[19] In fact the electronic structure of $Ba(Fe_{0.65}Ru_{0.35})_2As_2$ can be reasonably accounted for by LDA calculations with negligible electron correlation effects. This tendency is not observed for electron- or hole-doped compounds with similar T_c (Refs. 36, 39, and 40) and seems then to be a specific feature of this Ru-substituted system. One might reasonably think that these modifications would be at the origin of the evolution of the transport properties observed here.

Nevertheless the way how these band-structure modifications can also affect the strength of spin fluctuations or the carrier mobilities is not clear at present. Moreover, the resemblance displayed in Fig. 6 between the resistivity curves found for electrons and holes and those measured in electron- and hole-doped compounds appears very puzzling, as it suggests that the transport properties of electrons and holes are defined by their own and are not tightly dependent on the system of interest.

VI. CONCLUSION

The results presented here and in Ref. 19 clearly show that Ru is isovalent of Fe. We have confirmed that Ru substitution suppresses the magnetic state and induces superconductivity, which coexist in a given concentration range. Therefore it appears qualitatively very similar to the other types of substitutions.

From the structural point of view, we have shown that superconductivity can be induced although the $FeAs_4$ tetrahedra are strongly distorted on Ru addition. These structural modifications are in total contrast to those induced under pressure or by hole doping. This thus demonstrates that the regularization of tetrahedra cannot be the key structural factor for the occurrence of superconductivity as proposed recently.[8] However, we find that the relationship between the optimal T_c and the anion height above the Fe planes obeys the same plot as found for a lot of different iron-based compounds.[7] Even though this cannot be considered as the only parameter to drive superconductivity, this indicates that subtle details of crystal structure might tune specific properties of the Fermi surface necessary to optimize it.

We have demonstrated that a two-band model approach is a prerequisite to get insight into the respective contribution of electrons and holes to the transport properties of these multiband materials. Using combined studies of transport and ARPES measurements on the same samples, we have been able to disentangle the respective contributions of electrons and holes to transport properties. We have evidenced that their mobilities become comparable on Ru addition, even in the close proximity to magnetism. In addition, we find that the mobility of holes overcomes that of electrons at low T in superconducting samples. The observation that the $\rho(T)$ curves deduced for electrons and holes are very similar to those measured in electron- or hole-doped compounds suggests that the occurrence of optimal T_c in all these compounds is linked with well-defined features of the electron and hole bands. Further work, specifically studying the strength and the evolution of antiferromagnetic spin fluctuations with Ru contents, will hopefully allow to clarify the incidence of spin fluctuations, electronic correlations and filling of the electronic bands on the transport properties of these compounds.

ACKNOWLEDGMENTS

We would like to acknowledge H. Alloul and V. Brouet for fruitful discussions and critical reading of the manuscript.

*florence.albenque-rullier@cea.fr

[1] For a review, see I. I. Mazin and J. Schmalian, Physica C **469**, 614 (2009).

[2] M. Rotter, M. Tegel, and D. Johrendt, Phys. Rev. Lett. **101**, 107006 (2008).

[3] A. S. Sefat, R. Jin, M. A. McGuire, B. C. Sales, D. J. Singh, and D. Mandrus, Phys. Rev. Lett. **101**, 117004 (2008); A. Leithe-Jasper, W. Schnelle, C. Geibel, and H. Rosner, *ibid.* **101**, 207004 (2008); N. Ni, M. E. Tillman, J.-Q. Yan, A. Kracher, S. T. Hannahs, S. L. Bud'ko, and P. C. Canfield, Phys. Rev. B **78**, 214515 (2008).

[4] J.-H. Chu, J. G. Analytis, C. Kucharczyk, and I. R. Fisher, Phys. Rev. B **79**, 014506 (2009).

[5] Z. Ren, Q. Tao, S. Jiang, C. Feng, C. Wang, J. Dai, G. Cao, and Z. Xu, Phys. Rev. Lett. **102**, 137002 (2009).

[6] P. L. Alireza, Y. T. Chris Ko, J. Gillett, C. M. Petrone, J. M. Cole, S. E. Sebastian, and G. G. Lonzarich, J. Phys.: Condens. Matter **21**, 012208 (2009).

[7] Y. Mizugushi, Y. Hara, K. Deguchi, S. Tsuda1, T. Yamaguchi, K. Takeda, H. Kotegawa, H. Tou, and Y. Takano, arXiv:1001.1801 (unpublished).

[8] S. A. J. Kimber, A. Kreyssig, Y. Zhang, H. O. Jeschke, R. Valent, F. Yokaichiya, E. Colombier, J. Yan, T. C. Hansen, T. Chatterji, R. J. McQueeney, P. C. Caneld, A. I. Goldman, and D. N. Argyriou, Nature Mater. **8**, 471 (2009).

[9] P. Canfield and S. Bud'ko, arXiv:1002.0858, Condens. Matter Phys. (to be published).

[10] F. Rullier-Albenque, D. Colson, A. Forget, and H. Alloul, Phys. Rev. Lett. **103**, 057001 (2009).

[11] L. Fang, H. Luo, P. Cheng, Z. Wang, Y. Jia, G. Mu, B. Shen, I. I. Mazin, L. Shan, C. Ren, and H.-H. Wen, Phys. Rev. B **80**, 140508(R) (2009).

[12] E. van Heumen, Y. Huang, S. de Jong, A. Kuzmenko, M. Golden, and D. van der Marel, arXiv:0912.0636 (unpublished).

[13] S. Kasahara, T. Shibauchi, K. Hashimoto, K. Ikada, S. Tonegawa, R. Okazaki, H. Ikeda, H. Takeya, K. Hirata, T. Terashima, and Y. Matsuda, arXiv:0905.4427 (unpublished).

[14] H. Q. Luo, P. Cheng, Z. S. Wang, H. Yang, Y. Jia, L. Fang, C. Ren, L. Shan, and H. H. Wen, Physica C **469**, 477 (2009).

[15] A. S. Sefat, D. J. Singh, L. H. VanBebber, Y. Mozharivskyj, M. A. McGuire, R. Jin, B. C. Sales, V. Keppens, and D. Mandrus, Phys. Rev. B **79**, 224524 (2009).

[16] S. Sharma, A. Bharathi, S. Chandra, R. Reddy, S. Paulraj, A. Satya, V. Sastry, A. Gupta, and C. Sundar, Phys. Rev. B **81**, 174512 (2010).

[17] W. Schnelle, A. Leithe-Jasper, R. Gumeniuk, U. Burkhardt, D. Kasinathan, and H. Rosner, Phys. Rev. B **79**, 214516 (2009).

[18] L. Zhang and D. J. Singh, Phys. Rev. **79**, 174530 (2009).

[19] V. Brouet, F. Rullier-Albenque, M. Marsi, B. Mansart, J. Faure, L. Perfetti, A. Taleb-Ibrahimi, P. Le Fèvre, F. Bertran, A. Forget, and D. Colson, arXiv:1002.4952 (unpublished).

[20] R. W. W. Hooft, COLLECT, Nonius BV, Delft, The Netherlands (1998).

[21] Z. Otwinowski and W. Minor, Methods Enzymol. **276**, 307 (1997).

[22] G. M. Sheldrick, Acta Crystallogr., Sect. A: Found. Crystallogr. **64**, 112 (2008).

[23] $R_1=\Sigma||F_0|-|F_c||/\Sigma|F_0|$ $wR_2=\{\Sigma[w(F_0^2-F_c^2)^2]/\Sigma[w(F_0^2)^2]\}^{1/2}$, where the weighting scheme $w=1/[\sigma^2(F_0^2)+(aP)^2+bP]$ and $P=[2F_c^2+\max(F_0^2,0)]/3$, a and b being refined parameters.

[24] M. Rotter, M. Pangerl, M. Tegel, and D. Johrendt, Angew. Chem., Int. Ed. **47**, 7949 (2008).

[25] L. J. van der Pauw, Philips Res. Rep. **13**, 1 (1958).

[26] M. Rotter, M. Tegel, D. Johrendt, I. Schellenberg, W. Hermes, and R. Pöttgen, Phys. Rev. B **78**, 020503(R) (2008); X. F. Wang, T. Wu, G. Wu, H. Chen, Y. L. Xie, J. J. Ying, Y. J. Yan, R. H. Liu, and X. H. Chen, Phys. Rev. Lett. **102**, 117005 (2009).

[27] D. K. Pratt, W. Tian, A. Kreyssig, J. L. Zarestky, S. Nandi, N. Ni, S. L. Bud'ko, P. C. Canfield, A. I. Goldman, and R. J. McQueeney, Phys. Rev. Lett. **103**, 087001 (2009).

[28] Y. Laplace, J. Bobroff, F. Rullier-Albenque, D. Colson, and A. Forget, Phys. Rev. B **80**, 140501(R) (2009).

[29] T. Goko, A. A. Aczel, E. Baggio-Saitovitch, S. L. Bud'ko, P. C. Canfield, J. P. Carlo, G. F. Chen, P. Dai, A. C. Hamann, W. Z. Hu, H. Kageyama, G. M. Luke, J. L. Luo, B. Nachumi, N. Ni, D. Reznik, D. R. Sanchez-Candela, A. T. Savici, K. J. Sikes, N. L. Wang, C. R. Wiebe, T. J. Williams, T. Yamamoto, W. Yu, and Y. J. Uemura, Phys. Rev. B **80**, 024508 (2009).

[30] H. Fukazawa, T. Yamazaki, K. Kondo, Y. Kohori, N. Takeshita, P. M. Shirage, K. Kihou, K. Miyazawa, H. Kito, H. Eisaki, and A. Iyo, J. Phys. Soc. Jpn. **78**, 033704 (2009).

[31] C.-H. Lee, A. Iyo, H. Eisaki, H. Kito, M. T. Fernandez-Diaz, T. Ito, K. Kihou, H. Matsuhata, M. Braden, and K. Yamada, J. Phys. Soc. Jpn. **77**, 083704 (2008).

[32] J. Zhao, Q. Huang, C. De La Cruz, S. Li, J. W. Lynn, Y. Chen, M. A. Green, G. F. Chen, G. Li, Z. Li, J. L. Luo, N. L. Wang, and P. Dai, Nature Mater. **7**, 953 (2008).

[33] M. A. McGuire, D. J. Singh, A. S. Sefat, B. C. Sales, and D. Mandrus, J. Solid State Chem. **182**, 2326 (2009).

[34] V. Vildosola, L. Pourovskii, R. Arita, S. Biermann, and A. Georges, Phys. Rev. B **78**, 064518 (2008).

[35] Below $T_{S\text{-}M}$, the Hall resistivity is no longer linear with magnetic field. The Hall coefficient is then defined as: $R_H=\rho_{xy}(14T)/14$.

[36] V. Brouet, M. Marsi, B. Mansart, A. Nicolaou, A. Taleb-Ibrahimi, P. Le Fèvre, F. Bertran, F. Rullier-Albenque, A. Forget, and D. Colson, Phys. Rev. B **80**, 165115 (2009).

[37] N. Doiron-Leyraud, P. Auban-Senzier, S. Rene de Cotret, C. Bourbonnais, D. Jérome, K. Bechgaard, and L. Taillefer, Phys. Rev. B **80**, 214531 (2009).

[38] F. Ma, Z. Lu, and T. Xiang, Front. Phys. China **5**(2), 150 (2010).

[39] H. Ding, K. Nakayama, P. Richard, S. Souma, T. Sato, T. Takahashi, M. Neupane, Y. Xu, Z. Pan, A. Federov, Z. Wang, X. Dai, Z. Fang, G. Chen, J. Luo, and N. Wang, arXiv:0812.0534 (unpublished).

[40] M. Yi, D. H. Lu, J. G. Analytis, J.-H. Chu, S.-K. Mo, R.-H. He, R. G. Moore, X. J. Zhou, G. F. Chen, J. L. Luo, N. L. Wang, Z. Hussain, D. J. Singh, I. R. Fisher, and Z.-X. Shen, Phys. Rev. **80**, 024515 (2009).